

Magnetic structure of free iron clusters compared to iron crystal surfaces

O. Šipr

Institute of Physics, Academy of Sciences of the Czech Republic, Cukrovarnická 10, CZ-162 53 Prague, Czech Republic

M. Košuth and H. Ebert

Universität München, Department Chemie, Butenandtstrasse 5-13, D-81377 München, Germany

(Received 5 May 2004; revised manuscript received 10 August 2004; published 15 November 2004)

Electronic and magnetic properties of free Fe clusters of 9 to 89 atoms are investigated theoretically within an *ab initio* fully relativistic framework and compared to results of crystal surfaces. It is found that the local spin magnetic moments μ_{spin} and the orbital magnetic moments μ_{orb} are enhanced for atoms close to the surface of a Fe cluster. The corresponding Friedel-like oscillations in the depth profiles of μ_{spin} and μ_{orb} are more pronounced for clusters than for crystal surfaces. The μ_{spin} in clusters and at crystal surfaces turned out to depend linearly on the effective coordination number N_{eff} . This empirical $\mu_{\text{spin}}-N_{\text{eff}}$ inter-relationship is able to account for some features of the experimentally measured dependence of the magnetic moment of free Fe clusters on the cluster size. The spin-polarized density of states (DOS's) for atoms in clusters is characterized by sharp atomlike peaks and substantially differs from the DOS in the bulk. The width of the local valence band gets more narrow if one is moving from the center of the cluster to its surface. The DOS averaged over all atoms in a cluster converges to the bulk behavior more quickly with cluster size than the DOS of the central atoms of these clusters.

DOI: 10.1103/PhysRevB.70.174423

PACS number(s): 75.75.+a, 73.22.Dj, 71.15.Rf

I. INTRODUCTION

Clusters comprising few tens or hundreds of atoms form an interesting class of materials, because they form a bridge between atoms and molecules, on the one hand, and solids, on the other, and yet their properties cannot be described by a simple interpolation between the two extremes. Consequently, magnetic properties of transition metal clusters attracted a lot of attention—both due to fundamental reasons and due to a potential application in magnetic recording industry. As clusters contain a large portion of surface atoms, it is interesting to study the relation between the electronic and magnetic properties of atoms which are close to a cluster surface and of atoms which are close to a planar surface of a crystal. Although the importance of surface-related effects in clusters has been universally acknowledged, no systematic study comparing clusters and crystal surfaces has been performed so far to the best of our knowledge. The aim of this work is thus to focus on theoretical investigations of free iron clusters with bcc geometry and bulk interatomic distances and on comparing their properties with properties of bcc-Fe crystal surfaces.

Previous work on free medium-sized Fe clusters of 10–100 atoms with a geometry taken as if cut from the bulk relied mostly on a parametrized tight-binding (TB) model Hubbard Hamiltonian.^{1–3} Early *ab initio* calculations, on the other hand, were restricted to Fe clusters containing not more than 15 atoms.^{4–6} More recent work relying on an *ab initio* approach have focused mainly on geometry optimization of small or medium-sized clusters^{7,8} and thus cannot be directly utilized for comparing with crystal surfaces. Generally, nearly all calculations of electronic structure of free metallic clusters were non relativistic, meaning that they do not give access to the orbital contribution to the magnetic moment. Only recently orbital magnetic moments for free Ni clusters

obtained by means of TB model calculations with spin-orbit coupling included via an intra-atomic approximation were presented.⁹ Preliminary results of fully relativistic *ab initio* calculations of spin magnetic moments μ_{spin} and of orbital magnetic moments μ_{orb} of free Fe clusters were published by the present authors.¹⁰

Several calculations of the dependence of μ_{spin} on the depth below the crystal surface have been published for bcc Fe, using an *ab initio* formalism^{11–17} as well as a TB model Hamiltonian.¹⁸ Most of these investigations deal with the (001) surface; less work has been done on the (110) surface and only little attention has been devoted to the (111) surface. Similarly as in the case of clusters, not many papers include μ_{orb} in their consideration. *Ab initio* calculations of the profile of μ_{orb} were published for a perpendicularly magnetized (001) surface,^{13,17,19} a systematic study of the orbital magnetism below surfaces of transition metals was performed by Rodríguez-López *et al.*¹⁸

Magnetic moments of free iron clusters were measured by Stern-Gerlach-type experiments.²⁰ It was found that the total magnetic moment of clusters per one atom oscillates with the size of the cluster, approaching only slowly its bulk value. Several attempts were made to reproduce this oscillatory dependence either via calculating magnetic moments at each site of a given cluster^{3,21} or via simple models relying on the atomic shell structure of respective clusters,^{22–24} with partial success.

In principle, μ_{spin} and μ_{orb} can be measured separately by means of the x-ray magnetic circular dichroism (XMCD) of x-ray absorption spectra, via a judicious use of sum rules.²⁵ Several experimental studies were performed on *supported* iron clusters.^{26–28} These studies suggest a substantial enhancement of μ_{orb} as well as of the ratio between μ_{orb} and μ_{spin} with respect to the bulk, while μ_{spin} remains the same as in the bulk or even decreases.

The purpose of this paper is to investigate theoretically magnetic properties of free iron clusters. We start with describing our fully relativistic *ab initio* computational formalism. Then the dependence of μ_{spin} and μ_{orb} on the distance of atomic sites from the cluster center and the dependence of μ_{orb} on the direction of the magnetization is discussed for several cluster sizes. This is followed by a comparison of the magnetic properties of atoms in free clusters to properties of atoms at and below crystal surfaces. Then we study systematic trends of magnetic moments in clusters and at surfaces and in particular their dependence on the effective coordination number. This dependence is then utilized for estimating the magnetic moments of large clusters and a subsequent comparison of our results with experimental data. Finally, spin-polarized densities of states (DOS) of iron atoms in clusters are analyzed.

II. THEORETICAL METHODS

We investigate free spherical-like clusters constructed from 1–7 coordination shells of bulk bcc Fe (lattice constant $a=2.87$ Å). Our neglect of the geometry relaxation is most serious for small clusters, which in reality may adopt various structures with sometimes tiny differences in their total energies.^{7,29} The structure of larger clusters seems to be less effected by geometry relaxation, as suggested by TB model Hamiltonian calculations^{1,30} as well as by *ab initio* results.⁸ In contrast to the previous work, our study primarily focuses on comparing spin and orbital contributions to cluster and surface magnetism, in particular for relatively large clusters. The neglect of the geometry relaxation for both type of systems seems to be adequate because it allows a more direct comparison.

Our theoretical investigations are based on the local spin density approximation (LSDA) scheme to deal with exchange and correlation effects. The Vosko, Wilk, and Nusair parametrization of the exchange-correlation potential was used.³¹ The reliance on LSDA as opposed to the generalized gradient approximation (GGA) is justified in our study because we focus on magnetic properties of fixed-geometry systems. Although GGA was found to be superior to LSDA in exploring structural properties of transition metals,³² its benefit in magnetic studies is still questionable.^{33–35}

The electronic and magnetic structure of clusters was calculated in real space via a fully relativistic spin-polarized multiple-scattering technique,³⁶ as implemented in the SPRKKR code.³⁷ We relied on spherical potentials in the atomic sphere approximation (ASA). In order to account for the spilling of the electron charge into the vacuum, the clusters were surrounded by empty spheres. The scattering potential of atoms in the clusters was obtained from scalar-relativistic self-consistent-field (SCF) calculations for clusters using an amended XASCF code.^{38,39} Use of scalar-relativistic potentials was in fact not crucial in our study: we found that results of our fully relativistic calculation of the electronic structure do not change if the scattering potential is taken from a nonrelativistic SCF calculation instead of from a scalar-relativistic one. Some further technical details on our way of constructing the cluster potential can be found in Ref. 40.

Crystal surfaces were simulated by finite 2D slabs, again with bulk interatomic distances throughout the whole system. For the (001) surface, we used 18 planes of Fe atoms and 7 planes with empty spheres on both sides of the iron slab, for the (110) surface we used 18 planes of Fe atoms and 6 planes with empty spheres, and for the (111) surface we used 34 planes of Fe atoms and 7 planes with empty spheres. The electronic and magnetic structure of these slabs was calculated via a fully relativistic spin-polarized tight-binding (TB) Korringa-Kohn-Rostoker (KKR) method.^{41,42} Similarly as in the case of free clusters, the potential was taken in the ASA form. We checked that the convergence to bulk properties was achieved in the central layers.

All calculations have been done assuming a collinear spin configuration, i.e., the orientation of the magnetization is characterized by a common vector \mathbf{M} . This restriction might be questionable for the clusters because, in this case, noncollinear spin structures for the ground state have indeed been found for very small Fe clusters (containing up to five atoms).^{43,44} Test calculations done for a Fe cluster with 9 atoms using the VASP code⁴⁵ lead to a collinear spin configuration.⁴⁶ Because also all other clusters studied within this investigation had a highly symmetric cubic geometric structure with closed atomic shells, it is expected that assuming a collinear spin structure is well justified.

III. RESULTS AND DISCUSSION

A. Magnetic profiles of free clusters

The dependence of μ_{spin} on the distance of atomic sites from the cluster center is displayed in Fig. 1, for cluster sizes ranging from 9 atoms (a single coordination shell) to 89 atoms (seven coordination shells around the central atom). In contrast to a nonrelativistic or scalar-relativistic description, atoms belonging to the same coordination shell need not be all symmetry equivalent, because the presence of a magnetization and of spin-orbit coupling lowers the symmetry of our systems.⁴⁷ Nevertheless, it can be seen from Fig. 1 that the *spin* magnetic moments of atoms of the same coordination shell are practically all identical, even if they are inequivalent due to the presence of spin-orbit coupling (small differences can be observed only for atoms in the outermost shell of the 65-atoms cluster). Likewise, there is practically no dependence of μ_{spin} on the direction of the magnetization, in line with previous findings, e.g., for bulk systems.⁴⁸ This behavior can be explained by the fact that the spin magnetic moment is determined by the difference in the populations of the exchange-split spin up and spin down states, that is hardly changed if the spin-orbit coupling is considered as a perturbation.

On the other hand, μ_{orb} exhibits quite a strong dependence both on the symmetry class of the atoms within a coordination shell and on the direction of the magnetization. This can be seen in Fig. 2, where the profiles in μ_{orb} are shown for three magnetization directions (the magnetization \mathbf{M} is parallel to one of the [001], [110], and [111] crystallographic directions). The spread in values of μ_{orb} for inequivalent atoms of the same coordination shell clearly differs from one cluster to another, with no obvious systematic dependence on

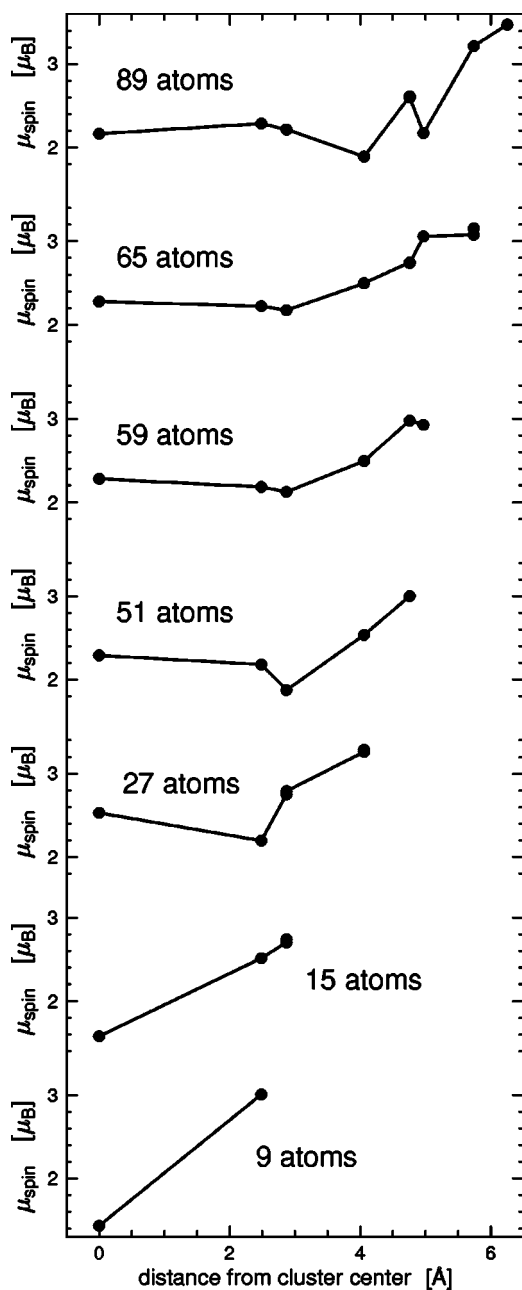


FIG. 1. Dependence of μ_{spin} in free iron clusters on the distance of the atoms from the center of the cluster. Each cluster is identified by the number of constituting atoms.

the cluster size (the spread is small for clusters of 15 and 51 atoms but quite large for clusters of 9, 27, or 89 atoms). Note that the lowering of cluster symmetry induced by the magnetization depends on the direction of M , meaning that the number of symmetry inequivalent classes into which atoms of the same coordination shell split may be different for different magnetization directions, as it can also be observed in Fig. 2. In line with this, we find that the spread of μ_{orb} within an atomic shell is smallest for M oriented along the high-symmetry direction ([001]) while it is in general largest for M coincident with the direction of the lowest symmetry ([110]).

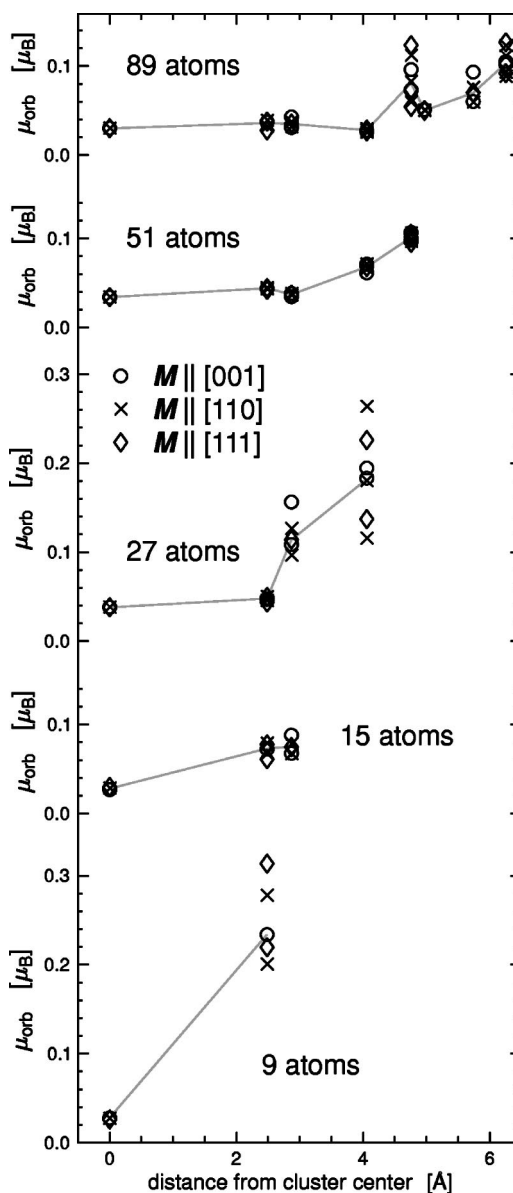


FIG. 2. μ_{orb} in free iron clusters as a function of the distance of the atoms from the center (point marks). The magnetization M is oriented parallel to the [001], [110], or [111] crystallographic directions, as indicated in the legend. The solid lines denote μ_{orb} averaged over all atoms in a coordination shell. Each cluster is identified by the number of constituting atoms.

It can be deduced from Figs. 1 and 2 that both μ_{spin} and μ_{orb} are enhanced when approaching a cluster surface. This enhancement does *not* monotonously depend on the distance. Rather, Friedel-like oscillations in μ_{spin} and μ_{orb} appear. At some sites, μ_{spin} or μ_{orb} may acquire values which are lower than those at the central atom. Convergence of μ_{spin} and μ_{orb} to bulk values has not yet been attained even at the center of the 89-atoms cluster (our SPRKKR calculations yields bulk values of $2.28\mu_B$ for μ_{spin} and $0.054\mu_B$ for μ_{orb}).

Although μ_{orb} at individual atoms may depend quite strongly on the magnetization direction, μ_{orb} averaged over all atoms of a given coordination shell (shown via lines in Fig. 2) does not exhibit any significant dependence on the

TABLE I. Magnetic properties of iron clusters averaged over all their atoms as a function of cluster size. The first column displays the number of atoms in a cluster, the second and the third columns show average $\bar{\mu}_{\text{spin}}$ and $\bar{\mu}_{\text{orb}}$, the fourth column contains the ratio of averages $\bar{\mu}_{\text{orb}}/\bar{\mu}_{\text{spin}}$, and the last column shows the average number of holes in the d band.

Size	$\bar{\mu}_{\text{spin}}$ [μ_B]	$\bar{\mu}_{\text{orb}}$ [μ_B]	$\bar{\mu}_{\text{orb}}/\bar{\mu}_{\text{spin}}$	n_h
9	2.84	0.208	0.0731	2.89
15	2.54	0.070	0.0275	3.02
27	2.83	0.125	0.0441	3.19
51	2.62	0.075	0.0285	3.22
59	2.68	0.062	0.0233	3.27
65	2.66	0.074	0.0281	3.34
89	2.70	0.068	0.0253	3.34
bulk	2.28	0.054	0.0237	3.44

direction of the magnetic field. This suggests a very small magnetic anisotropy energy (MAE) for closed-shell spherical clusters,⁴⁹ of the same order as in the bulk. In this respect our clusters differ from smaller low-symmetry clusters investigated by Pastor *et al.*,⁵⁰ for which a MAE as large as in thin films has been found.

So far we were concerned with magnetic profiles, i.e., with the distribution of μ_{spin} and μ_{orb} within each cluster. However, experiment typically sees only values averaged over all atoms constituting a cluster. Therefore, we present in Table I total μ_{spin} and μ_{orb} of clusters divided by the number of atoms $\bar{\mu}_{\text{spin}}$, $\bar{\mu}_{\text{orb}}$ and also their ratio $\bar{\mu}_{\text{orb}}/\bar{\mu}_{\text{spin}}$. As the analysis of experimental XMCD spectra on the basis of the sum rules involves the average number of holes in the $3d$ band, this quantity is presented in Table I as well. We will focus on average cluster magnetic moments in Sec. III E in more detail. Here we would like only to note that Table I reveals that the $\bar{\mu}_{\text{orb}}/\bar{\mu}_{\text{spin}}$ ratio approaches the bulk value much more quickly than $\bar{\mu}_{\text{spin}}$ or $\bar{\mu}_{\text{orb}}$ separately. This might be seen as a contradiction to some experimental XMCD studies which suggest that the $\bar{\mu}_{\text{orb}}/\bar{\mu}_{\text{spin}}$ ratio is about twice as high for supported iron clusters than for the bulk Fe crystal.^{26–28} We suppose that one of the main reasons for this discrepancy rests in the shape of the clusters: supported clusters investigated in Refs. 26–28 were probably rather flat than spherical, containing thus a much larger portion of surface and edge atoms with a large μ_{orb} than the spherical clusters we investigate here. A further reason for the different dependency of the $\bar{\mu}_{\text{orb}}/\bar{\mu}_{\text{spin}}$ ratio given in Table I and deduced from the mentioned XMCD investigations is that relativistic calculations based on plain spin density functional theory give the spin-orbit-induced μ_{orb} often too small⁵¹ (see also Sec. III B). This problem is in fact more pronounced for small clusters than for the bulk.⁵² Finally, one has to mention that the estimate of $\bar{\mu}_{\text{spin}}$ on the basis of the sum rules is normally based on the assumption that the spin magnetic dipole term T_z in the sum rule can be ignored.⁵³ Our calculations show that, indeed, for free *spherical* Fe clusters the T_z term is negligible (typically, it is by three orders of magnitude smaller than μ_{spin}). However, for low-dimensional or

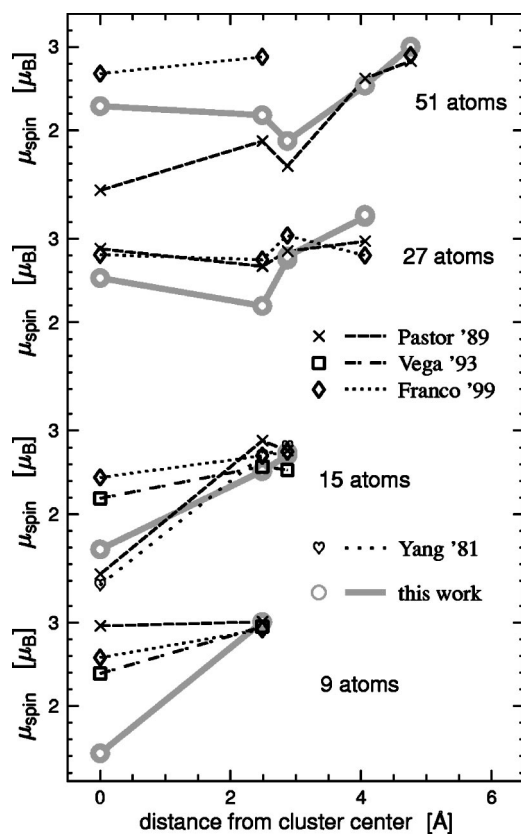
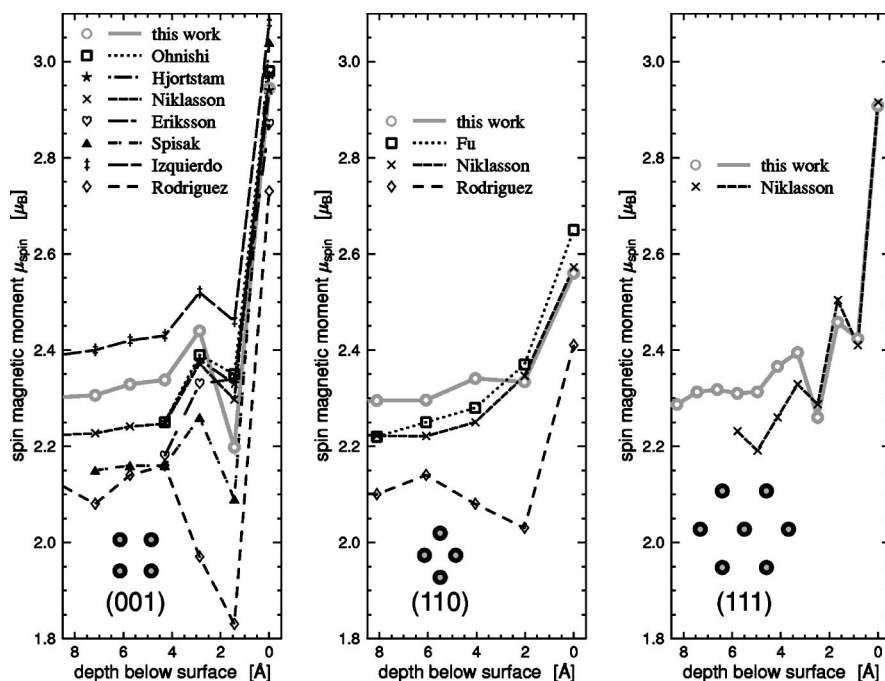


FIG. 3. Comparison of μ_{spin} profiles as calculated by different methods. Solid lines correspond to this work, coarsely dotted line to Yang *et al.* (Ref. 5), dashed line to Pastor *et al.* (Ref. 1), dash-dotted line to Vega *et al.* (Ref. 2), and densely dotted line to Franco *et al.* (Ref. 3). Each cluster is identified by the number of its atoms.

low-symmetry systems, the contribution coming from T_z may be significant.⁵⁴

It is worthwhile to compare our magnetic profiles with earlier work. In Fig. 3 we display our results together with μ_{spin} obtained from nonrelativistic SCF $X\alpha$ calculations of Yang *et al.*⁵ and from nonrelativistic parametrized model calculations of Pastor *et al.*,¹ Vega *et al.*,² and Franco *et al.*³ It is obvious from Fig. 3 that the spin magnetic profiles calculated by different methods show a rather pronounced spread. The differences are larger for the inner atoms than for the outer ones. This suggests that even without involving geometry optimization, the task of calculating electronic structure of metallic clusters is quite a complex one. On the other hand, in spite of the rather large quantitative scatter of the various results one nevertheless notices that the qualitative trend of the profiles is in reasonable agreement.

No other calculations of site-dependent μ_{orb} in free iron clusters have been published so far to the best of our knowledge. Guirado-López *et al.*⁹ presented recently results of their TB model Hamiltonian calculation of μ_{orb} in free spherical Ni clusters containing up to 165 atoms. Although our results for Fe clusters cannot be directly compared with results for Ni clusters, it is interesting to note that quite a significant dependence of μ_{orb} averaged over all atoms of a coordination shell on the magnetization direction was found by these authors, which is in contrast to the present results



for Fe clusters. It is conceivable that the local geometry of clusters is important in this respect: the Ni clusters investigated by Guirado-López *et al.*⁹ have either an fcc or an icosahedral structure while our Fe clusters have a bcc structure.

B. Magnetic profiles of crystal surfaces

In this section we display the results of our calculations of μ_{spin} and μ_{orb} at Fe crystal surfaces and compare them with available theoretical results obtained via different methods. Figure 4 summarizes the layer dependence of μ_{spin} for the (001), (110), and (111) crystal surfaces and compares them with full-potential linearized augmented plane wave method calculations of Ohnishi *et al.*¹¹ and Fu and Freeman,¹² Green's function linear-muffin-tin-orbital (LMTO) calculations of Niklasson *et al.*,¹⁵ LMTO calculations of Eriksson *et al.*,¹⁹ full-potential LMTO calculations of Hjortstam *et al.*,¹³ TB-LMTO calculations of Spišák and Hafner,¹⁴ linear combination of (pseudo) atomic orbitals calculations of Izquierdo *et al.*,¹⁶ and *d*-band model Hamiltonian calculations of Rodríguez-López *et al.*¹⁸

One can see that the basic trend, namely, a rather strong enhancement of μ_{spin} at crystal surfaces, is attained by all calculations. For the (110) surface this enhancement is significantly smaller than for the (001) and (111) surfaces; this is consistent with the fact that atoms at the (110) surface have higher coordination numbers than atoms at the other two surfaces. The increase of μ_{spin} with decreasing distance from the surface is usually not monotonous. It was suggested that these Friedel-like oscillations are an artifact caused by an insufficient number of layers involved in slab-type calculations.^{11,12} However, these oscillations persist even if the number of layers in which the electronic structure has been allowed to relax is as large as 9 or 10 (which is the case of our work or Ref. 15) and also when dealing with a semi-

FIG. 4. Layer dependence of μ_{spin} below the (001) Fe crystal surface (left panel), (110) crystal surface (middle panel), and (111) crystal surface (right panel). The surface structures are schematically depicted in the insets. Together with our results we display results of Ohnishi *et al.* (Ref. 11), Fu and Freeman (Ref. 12), Hjortstam *et al.* (Ref. 13), Niklasson *et al.* (Ref. 15), Eriksson *et al.* (Ref. 19), Spišák and Hafner (Ref. 14), Izquierdo *et al.* (Ref. 16), and Rodríguez-López *et al.* (Ref. 18), as indicated in the legend. The calculations of Ohnishi *et al.* (Ref. 11) and of Hjortstam *et al.* (Ref. 13) yield very similar results and span the same range of layers, so that the corresponding lines in the left panel are hard to distinguish from one another.

infinite crystal geometry.¹⁷ Likewise, these oscillations are present in ASA as well as in full-potential calculations^{11,13,16} so approximating the shape of the potential does not seem to be significant in this respect either. Note that full-potential KKR calculations confirmed that the ASA is a good approximation for calculating the electronic structure of Fe surfaces, as long as one is not interested in surface states that are relevant, e.g., in scanning-tunneling microscopy.⁵⁵ It appears therefore that the presence of Friedel-like oscillations in μ_{spin} below crystal surfaces is well confirmed.

In Fig. 5 we compare μ_{orb} at the (001) and (110) surfaces for the magnetization oriented either perpendicular or parallel to the surface, as computed by the fully relativistic TB-KKR approach (present work) and by the *d*-band model Hamiltonian calculations of Rodríguez-López *et al.*¹⁸ In the case of the (001) surface with perpendicular magnetization, LMTO calculations of Eriksson *et al.*¹⁹ and Hjortstam *et al.*¹³ are also displayed in the graph.

Our calculations do not include the so-called orbital polarization (OP) term that was introduced by Brooks to account for the enhancement of spin-orbit-induced μ_{orb} due to electronic correlations.^{56,57} As Hjortstam *et al.*¹³ present their results both with the OP term included and without it, we choose for comparison their results obtained without the OP term. Adding the orbital polarization term to the Hamiltonian is supposed to account heuristically for some many-body effects which give rise to the Hund's second rule in atomic theory and which are neglected by the local approximations to relativistic spin density functional theory.^{36,58} These essentially atomic many-body effects are presumably better described by the model Hamiltonian approach employed by Rodríguez-López *et al.*¹⁸ or by the LDA+*U* scheme.⁵⁹ In fact the LDA+*U* as well as the OP schemes can be combined with the fully relativistic spin-polarized KKR formalism used here for the electronic structure calculations.^{58,60} As the present study primarily aims to investigate the dependency

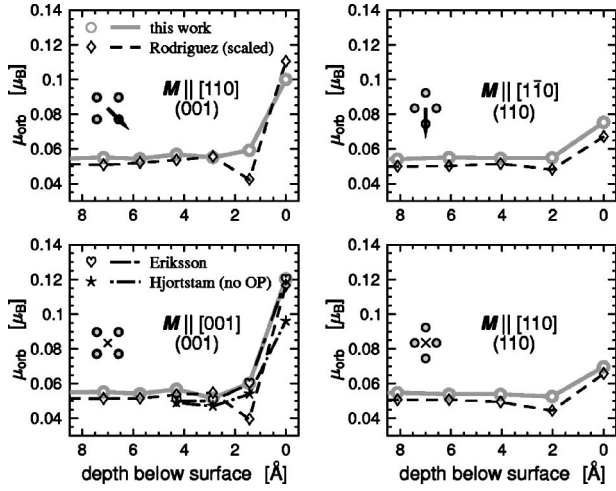


FIG. 5. Layer-dependence of μ_{orb} below iron crystal surfaces; left panels stand for the (001) surface, right panels for the (110) surface. The magnetization \mathbf{M} is either perpendicular (lower panels) or parallel (upper panels) to the surface, its orientation is schematically depicted in the insets. Moments calculated by Rodríguez-López *et al.* (Ref. 18) (scaled by a factor of 0.57) and in the case of the (001) surface with perpendicular magnetization also by Eriksson *et al.* (Ref. 19) and by Hjortstam *et al.* (Ref. 13) (without OP) are shown for comparison. The results of Eriksson *et al.* (Ref. 19) nearly coincide with our results, hence the corresponding line is hard to distinguish in the lower left panel.

of local magnetic properties of closed-shell Fe clusters on their size and to compare these with their counterparts for corresponding surfaces, we restricted ourselves to plain LSDA-based calculations. Accordingly, to allow for a comparison of our results for μ_{orb} with those of Rodríguez-López *et al.*,¹⁸ we scaled their data down by a factor of 0.57, which is the average ratio between μ_{orb} obtained without and with OP at and below the (001) surface in the work of Hjortstam *et al.*¹³

One can observe from Fig. 5 that all the calculations provide a very similar enhancement of μ_{orb} at crystal surfaces. Similarly as in the case of μ_{spin} , this enhancement is larger for the (001) surface than for the (110) surface. A good overall agreement between our results and the scaled results of Rodríguez-López *et al.*,¹⁸ for the two different surfaces, suggests that the effect of orbital polarization on μ_{orb} at different layers indeed can be roughly estimated by a common multiplicative factor.

C. Comparison between magnetic profiles of clusters and surfaces

Our calculations of μ_{spin} and μ_{orb} of free clusters and at crystal surfaces were performed within a common theoretical framework, relying on identical or very similar approximations and computational methods. Hence they are well suited for a comparative study of magnetic properties of atoms in free clusters and at crystal surfaces. For this purpose, we focus on an 89-atom spherical cluster and slice it into atomic layers so that these layers form parts of corresponding planes in the parental bcc crystal. The numbers of atoms in layers

TABLE II. Number of atoms constituting each layer formed when slicing an 89-atom spherical cluster into planes perpendicular to the [001], [110], and [111] crystallographic directions. The first layer is the outermost one, the last layer is always that one which contains the central atom.

Layer	No. of atoms in layer		
	[001]	110]	[111]
1	1	2	3
2	12	13	1
3	9	18	6
4	16	23	6
5	13		7
6			6
7			12
8			7

perpendicular to three common crystallographic directions are summarized in Table II. As atoms belonging to the same crystallographic layer in a cluster are not all equivalent, that atom which is most “centrally” located was selected to represent the whole plane. This choice was made because among all atoms in such a layer, the properties of this atom will resemble most the properties of atoms in the corresponding layer below a crystal surface. At the same time, one has to bear in mind that our comparison of crystal and cluster surfaces concerns the ideal nonrelaxed bcc structures. Real clusters will probably have surface faces and interatomic distances different from those of crystal cuts.

The dependence of μ_{spin} on the distance from the crystal surface and from the surface of an 89-atom cluster is shown in Fig. 6. The enhancement of μ_{spin} at the surface is larger in clusters than in crystals for all three directions we explored, which is consistent with a lower coordination number of the atoms at the surface of a cluster than at the surface of a crystal. The Friedel-like oscillations are more pronounced in the clusters than in the surface region of crystals. They appear to be in phase for the [110] and [111] directions but not for the [001] direction. This could be intuitively understood given the fact that for semi-infinite crystals, there is only an abrupt termination by the surface in one direction, while for clusters there are many such terminations. The oscillations of μ_{spin} in clusters can thus be viewed as arising from a complex interference of several Friedel-like oscillations. The different phase of the μ_{spin} oscillations for clusters and crystal surfaces in the [001] direction is thus not very surprising.

Layer-by-layer profiles of μ_{orb} for clusters and semi-infinite crystals are displayed in Fig. 7. The magnetization vector \mathbf{M} is either perpendicular to the layers (i.e., parallel to the direction in which the cluster and the semi-infinite crystal are probed) or parallel to the layers. In the case of the [110] probing direction, different profiles in μ_{orb} are obtained for different in-plane orientations of \mathbf{M} (middle panel of Fig. 7, dashed and dotted lines). For the [001] and [111] probing directions, no such dependence was found (the magnetic profiles for two mutually perpendicular in-plane directions of \mathbf{M} agree within a thickness of the line).

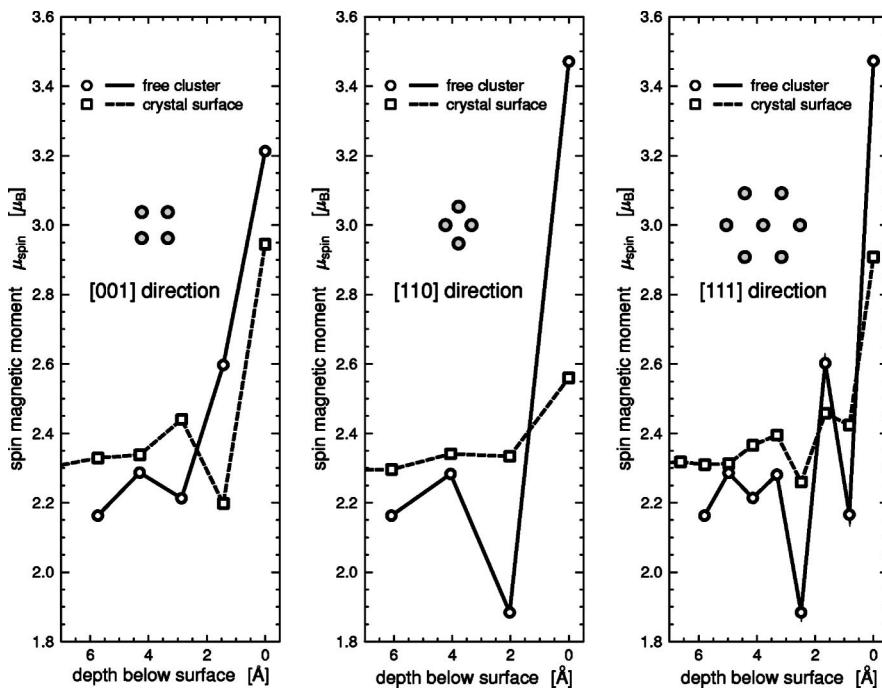


FIG. 6. μ_{spin} in an 89-atom cluster explored in the [001] (left panel), [110] (middle panel), and [111] (right panel) crystallographic directions compared with μ_{spin} at and below corresponding crystal surfaces.

The surface enhancement of μ_{orb} as well as Friedel-like oscillations are more pronounced at clusters than at surfaces. Similarly, the difference between μ_{orb} for \mathbf{M} perpendicular to the layers or parallel to them is larger at clusters than at surfaces. Note that this finding does not contradict our earlier statement that there is hardly any anisotropy in shell-averaged μ_{orb} (Sec. III A), because here we focus on μ_{orb} for individual atoms and not on average values.

D. Systematic trends in magnetic moments

The enhancement of μ_{spin} at surfaces is in general ascribed to the reduction of the coordination number of the surface atoms. According to tight-binding considerations, this leads to a narrowing of the electronic band and in turn in

general to an increase of the DOS at the Fermi level. On the basis of the Stoner criterion one finally expects an increase of μ_{spin} compared to the bulk system. Although isolated clusters—in contrast to a surface regime—have a discrete eigenvalue spectrum, this chain of arguments seems to be applicable for them as well. In fact, it has been shown by many examples that magnetic moments of atoms in transition metals increase if the atomic coordination number decreases.⁶¹ However, such a dependence has never been assessed in a quantitative way. Our study incorporates Fe atoms for quite a large range of coordination numbers. Exploring the dependence of μ_{spin} and μ_{orb} on the number of neighbors offers thus a natural way for analyzing the theoretical data we have obtained.

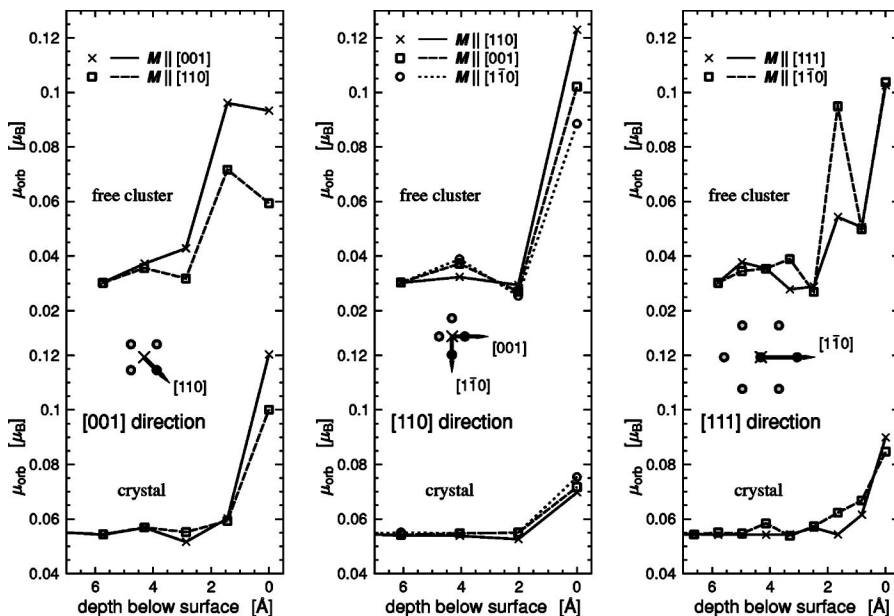


FIG. 7. μ_{orb} in an 89-atom cluster explored in the [001] (left panel), [110] (middle panel), and [111] (right panel) crystallographic directions compared with μ_{orb} at and below corresponding crystal surfaces. The magnetization is either perpendicular to the layers (solid lines) or parallel to them (dashed and dotted lines). For the case of an in-plane magnetization, the direction of the magnetic field \mathbf{M} is also indicated by the inset drawings. In each panel, the upper graph corresponds to the cluster while the lower graph to the semi-infinite crystal.

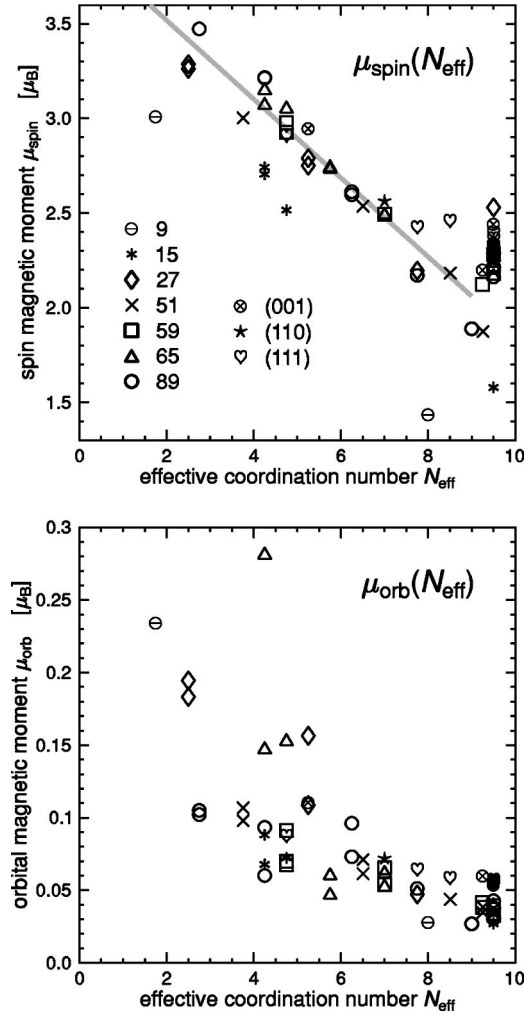


FIG. 8. μ_{spin} and μ_{orb} of atoms in clusters and at crystal surfaces as a function of the effective coordination number N_{eff} . Assignment of marks to different clusters and crystal surfaces is indicated by the legend in the upper panel. The straight line in the upper panel is a fit to the data in the region $N_{\text{eff}} < 8.5$, with the 9- and 15-atom clusters omitted.

In order to account for the influence of the nearest as well as the next-nearest neighbors, we rely on the effective coordination number N_{eff} (Ref. 62)

$$N_{\text{eff}} = N_1 + \beta N_2, \quad (1)$$

where N_1 is the number of the nearest neighbors and N_2 is the number of the next-nearest neighbors. The coefficient β is determined by the distance dependence of the d electron hopping integrals.^{62,63} Following Pastor *et al.*⁶³ and Zhao *et al.*,²³ we take $\beta=0.25$, meaning that we have $N_{\text{eff}}=9.50$ for atoms in a bulk system with bcc structure. We checked that the main conclusions drawn in this section are not very sensitive to the particular value of the β coefficient. Figure 8 summarizes μ_{spin} and μ_{orb} for all the cluster sizes and crystal surface types we explored as a function of N_{eff} . For clusters we consider μ_{orb} averaged over all atoms in a given shell (which are essentially independent of M , see Sec. III A), for crystal surfaces we make an average of μ_{orb} for in-plane and

perpendicular magnetizations. One can see that μ_{spin} depends on N_{eff} approximately in a linear way, especially if data points for the smallest clusters of 9 and 15 atoms are excluded. Fitting these data in the $N_{\text{eff}} < 8.5$ region, we arrive at the following relation:

$$\mu_{\text{spin}} = -0.21 \times N_{\text{eff}} + 3.94. \quad (2)$$

If we considered only atoms in clusters, the slope would be a bit more steeper ($\mu_{\text{spin}} = -0.22 \times N_{\text{eff}} + 3.98$), if we considered only atoms at crystal surfaces, the slope would be more moderate ($\mu_{\text{spin}} = -0.16 \times N_{\text{eff}} + 3.71$). Such a linear dependence describes $\mu_{\text{spin}}(N_{\text{eff}})$ only for $N_{\text{eff}} \leq 8.0$; for larger N_{eff} , μ_{spin} saturates around the bulk value with considerable deviations of individual data points from this mean value. Note that the linear dependence of μ_{spin} on N_{eff} revealed by Fig. 8 differs from the $\sim N_{\text{eff}}^{-1/2}$ form which was used in Refs. 23 and 24 and which follows from certain assumptions about the character of the DOS and exchange interaction (rectangular d band, second moment approximation, d -band splitting caused by exchange interaction same for clusters and bulk).

Similarly to the case of μ_{spin} , one can also observe an essentially monotonous decrease of μ_{orb} with increasing N_{eff} for both free clusters and crystal surfaces (lower panel of Fig. 8). However, one cannot describe this with a mathematically simple relationship as in Eq. (2) and also the spread of the values of μ_{orb} for a given N_{eff} is relatively large. Despite this fact, the correlation between μ_{orb} and N_{eff} is obvious, although less clear cut than in the case of μ_{spin} . This $\mu_{\text{orb}}-N_{\text{eff}}$ inter-relationship can be explained to some extent by an expression for the spin-orbit induced μ_{orb} that is based on perturbation theory and that relates μ_{orb} to the difference of the DOS at the Fermi level for the spin up and spin down components.¹⁷ Obviously, this difference will depend on the coordination number N_{eff} in a similar way as discussed above for the total DOS at the Fermi level.

The number of valence electrons of atoms in the surface region of a cluster or solid will in general be reduced because of the spill-out of electrons into the vacuum region. Due to the pronounced exchange splitting (see Sec. III F below) and the band narrowing discussed above this will primarily affect the minority-spin electrons. As a consequence, one may expect at least a monotonous variation of μ_{spin} with the number of valence electrons N_{val} for atoms in the surface region. In fact, as it can be seen in the upper panel of Fig. 9, a nearly linear relationship between μ_{spin} and N_{val} is found when plotting the data for the various systems considered here. In particular one finds, in line with the given arguments, that atoms in the (110), (001), and (111) surface layers of a semi-infinite Fe crystal with effective coordination numbers N_{eff} of 7.00, 5.25, and 4.75 exhibit a reduction of the number of valence electrons ΔN_{val} by -0.23 , -0.49 , and -0.62 compared to bulk, accompanied by an increase of μ_{spin} by 0.27, 0.65, and $0.61 \mu_B$, respectively. As can be seen from Fig. 9, the cluster data—including those for the 9- and 15-atom clusters—follow the trend of the crystal surfaces results. Fitting all the data points satisfying $N_{\text{val}} < 8.6$ by a straight line yields

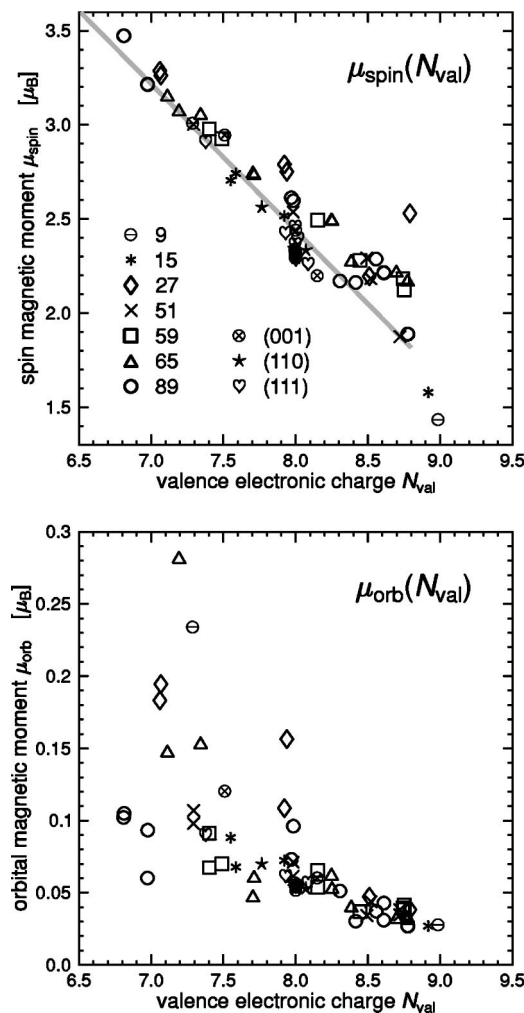


FIG. 9. μ_{spin} and μ_{orb} of atoms in clusters and at crystal surfaces as a function of the valence electronic charge N_{val} . Assignment of marks to different clusters and crystal surfaces is indicated by the legend in the upper panel. The straight line in the upper panel is a fit to the data in the region $N_{\text{val}} < 8.6$.

$$\mu_{\text{spin}} = -0.78 \times N_{\text{val}} + 8.67. \quad (3)$$

If one considers data points for clusters only, the slope of the line is more moderate ($\mu_{\text{spin}} = -0.68 \times N_{\text{val}} + 8.04$) while if one takes into account only crystal surfaces, the slope is steeper ($\mu_{\text{spin}} = -1.04 \times N_{\text{val}} + 10.64$). Similarly as in the case of N_{eff} , the dependence of μ_{orb} on N_{val} cannot be described by a simple formula, although a general tendency for increasing μ_{orb} if N_{val} decreases is evident in the lower panel of Fig. 9.

The systems we study are all bcc-like, with fixed interatomic distances, hence Figs. 8 and 9 show the net effect of varying the coordination numbers. In real free clusters, relaxation of interatomic distances will take place. In order to check to what extent the quasilinear $\mu_{\text{spin}}(N_{\text{eff}})$ dependence holds if variations in distances occur, we focus briefly on μ_{spin} of structurally relaxed free clusters as calculated via an *ab initio* nonrelativistic method based on numerical local orbitals in combination with norm-conserving pseudopotentials

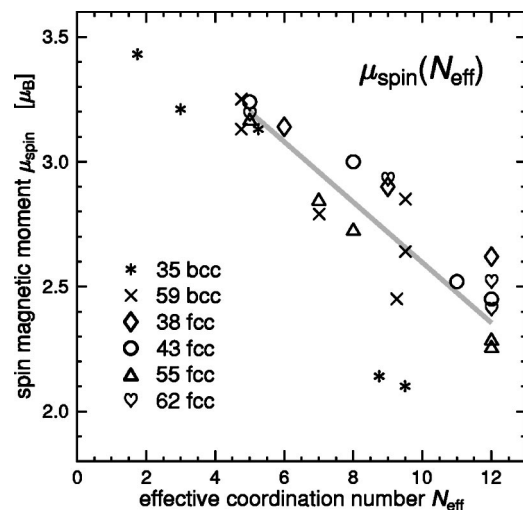


FIG. 10. μ_{spin} of atoms in structurally relaxed fcc-like and bcc-like clusters calculated by Postnikov *et al.* (Ref. 8) displayed as a function of N_{eff} . Assignment of marks to different clusters is indicated by the legend. The straight line is a fit to the data for fcc-like clusters.

by Postnikov *et al.*⁸ The clusters considered by these authors were either of bcc type (35 and 59 atoms) or of fcc type (38, 43, 55, and 62 atoms). The corresponding $\mu_{\text{spin}}(N_{\text{eff}})$ dependence for these six clusters is displayed in Fig. 10 [the β coefficient of Eq. (1) is taken zero for an fcc structure, according to Ref. 23]. It can be seen that the $\mu_{\text{spin}}-N_{\text{eff}}$ interrelationship retains its quasilinear character. Nevertheless, data points for the two bcc clusters noticeably deviate from the pattern set by the four fcc clusters. Data points for the fcc clusters give rise to the approximate relation

$$\mu_{\text{spin}} = -0.12 \times N_{\text{eff}} + 3.81, \quad (4)$$

which is also schematically depicted in Fig. 10. We can conclude that the approximately linear $\mu_{\text{spin}}(N_{\text{eff}})$ dependence seems to hold for structurally relaxed clusters as well, however, each structure type may have its own “best fit” coefficients.

E. Magnetic moments of large clusters

Since the experiment of Billas *et al.*,²⁰ a lot of effort has been devoted to explain the observed oscillations of the cluster magnetic moment per atom $\bar{\mu}_{\text{clu}}$ with cluster size. A proper theoretical approach would require calculating magnetic moments at each atomic site in the cluster. That is quite a formidable task; the largest iron clusters for which such a calculation has been done (relying on a TB model Hamiltonian) contained up to 200 atoms.^{3,21} For clusters containing several hundreds or thousands of atoms only model estimates can be done. Jensen and Bennemann,²² Zhao *et al.*,²³ and Aguilera-Granja *et al.*²⁴ calculated $\bar{\mu}_{\text{clu}}$ of clusters containing up to thousand of atoms for several cluster growth modes, making various assumptions about the dependence of magnetic moments on the local atomic environment. The depen-

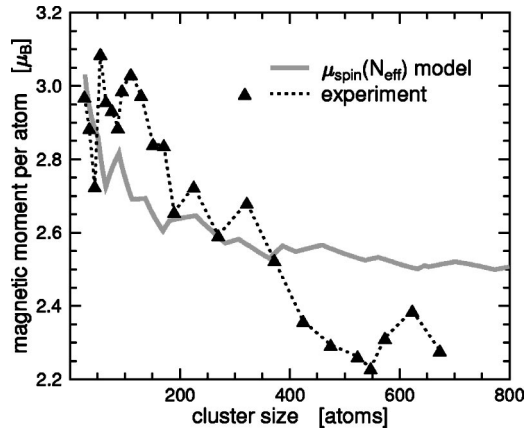


FIG. 11. Cluster magnetic moment per atom $\bar{\mu}_{\text{clu}}$ as a function of the cluster size, as calculated via a model $\mu_{\text{spin}}(N_{\text{eff}})$ dependence based on Eq. (2). The experiment of Billas *et al.* (Ref. 20) is shown for comparison.

dence of μ_{spin} and μ_{orb} on N_{eff} explored in the previous section makes it possible to make such calculations with far less free parameters.

As an illustration, we present in Fig. 11 $\bar{\mu}_{\text{clu}}$ calculated for clusters formed by spherical sections of the underlying bcc lattice. We assume that clusters grow by filling successive coordination shells. Within a particular coordination shell, new atoms get adsorbed at such sites that their N_{eff} is the highest possible (we found that the particular order in which the sites of yet unfilled coordination sphere are occupied is not crucial). Local μ_{spin} is taken from Eq. (2) for $N_{\text{eff}} < 8$, for larger N_{eff} we take the calculated value of bulk Fe ($2.28\mu_B$) instead. Similarly, μ_{orb} is calculated as $\mu_{\text{orb}} = -0.017N_{\text{eff}} + 0.19$ (linear fit to the lower panel of Fig. 8) for $N_{\text{eff}} < 8$ and the calculated bulk value of $0.054\mu_B$ is taken otherwise. As noted in Sec. III D, the linear fit does not describe μ_{orb} very accurately, however, we found that the total moment $\bar{\mu}_{\text{clu}}$ is not really sensitive to the orbital contribution—it just causes a more-or-less uniform increase of $\bar{\mu}_{\text{clu}}$ by about $0.05\mu_B$, independently of the cluster size.

It follows from Fig. 11 that this simple model accounts for some trends of the experiment. In particular, it is able to reproduce the three large oscillations in $\bar{\mu}_{\text{clu}}$ with peaks around 110 atoms, 210 atoms, and 320 atoms. For large cluster sizes, the model predicts that the bulk value of $\bar{\mu}_{\text{clu}}$ ought

to be approached as reciprocal of the third root of the number of atoms in a cluster. One would thus need 2500 atoms in order to approach the bulk $\bar{\mu}_{\text{clu}}$ up to $0.10\mu_B$ or 17000 atoms in order to approach bulk $\bar{\mu}_{\text{clu}}$ up to $0.05\mu_B$. On the other hand, experiment suggests that the bulk limit may be reached for smaller clusters (although this is hard to extrapolate as the measured $\bar{\mu}_{\text{clu}}$ still oscillates even for the largest clusters studied). The inability to describe the steep decrease of $\bar{\mu}_{\text{clu}}$ for clusters larger than ~ 400 atoms is a common feature of all semiphenomenological models.^{22–24}

The amplitudes of the $\bar{\mu}_{\text{clu}}$ oscillations provided by our model are smaller than in experiment (Fig. 11). Possibly, this may be connected with a wrong shape of our clusters. Several other shapes such as cube, octahedron, etc. could be considered. It is conceivable that the experiment actually probes a mixture of different shapes for a given cluster size. At the same time, one has to bear in mind that an earlier study of Jensen and Bennemann²² showed little sensitivity of the overall $\bar{\mu}_{\text{clu}}$ curve towards the cluster shape.

F. Spin-polarized densities of states

Local magnetic moments μ_{spin} and μ_{orb} carry integral information about the electronic structure. More specific details can be revealed through studying spin-polarized densities of states. Figure 12 displays the DOS at the central atom of 9-atom, 27-atom, and 89-atom clusters. For comparison, we show also the DOS for bulk Fe in each panel. The same energy-broadening (incorporated via a constant imaginary energy of 0.01 Ry) was applied both for clusters and for bulk. We found that the direction of the magnetic field has practically no influence on the DOS as displayed in this scale (different directions of \mathbf{M} yield DOS curves which are identical within the thickness of the line). Our results for the atom in the center of the 27-atom cluster moderately agree with model Hamiltonian results of Pastor *et al.*¹

Not surprisingly, the atom at the center of a 9-atom cluster displays quite sharp “atomiclike” features in the DOS.^{1,5} If the cluster size increases, the DOS gets smoother and a resemblance with the bulk gradually emerges. However, even for an 89-atom cluster the DOS for the central atom still differs considerably from the bulk—not only because of a sharper shape of the peaks but also concerning peak positions. Let us recall that it was found in Sec. III A that μ_{spin} and μ_{orb} at the central atom do not fully converge to their

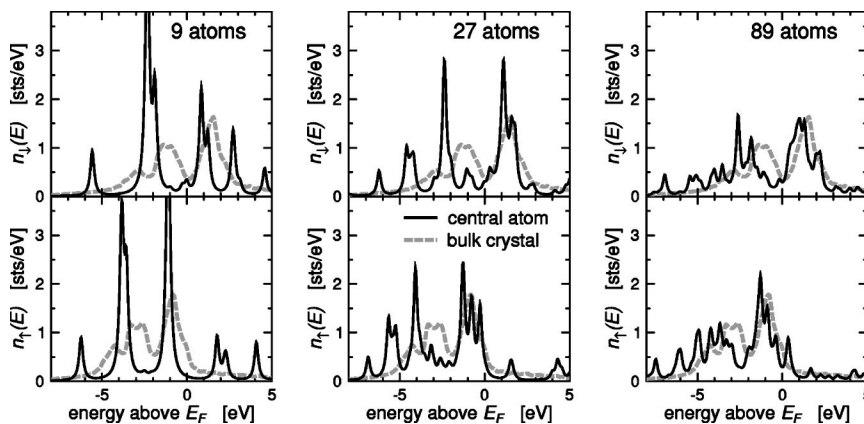


FIG. 12. Spin-polarized DOS at the central atom of a free Fe cluster (thin solid lines) and for an atom in bulk Fe (thick dashed lines). The left panel displays results for a 9-atom cluster, the middle panel for a 27-atom cluster and the right panel for an 89-atom cluster.

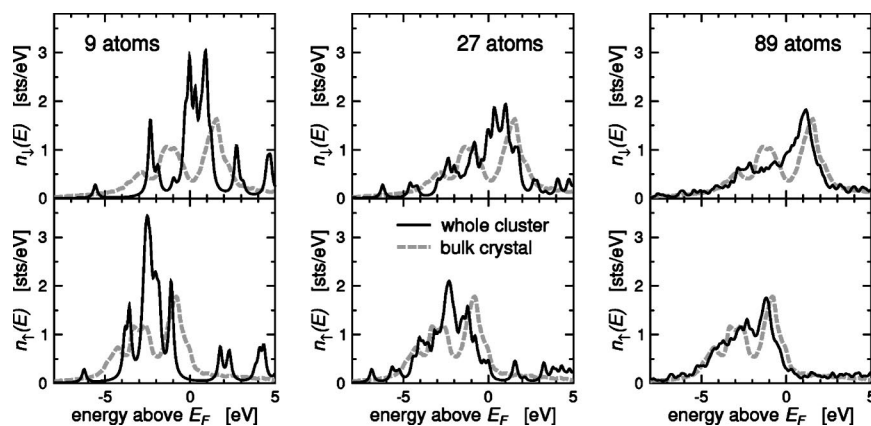


FIG. 13. Spin-polarized DOS averaged over all atoms of a free Fe cluster of 9, 27, and 89 atoms (thin solid lines) compared with the DOS of bulk Fe (thick dashed lines).

bulk values even at this cluster size. Through the DOS analysis, the relatively slow convergence of the electronic properties of clusters to bulk shows once more again.

By summing the DOS at all atoms in a cluster and dividing it subsequently by the number of atoms involved, one gets an (average) density of states of the whole cluster. It is displayed in Fig. 13 for three representative cluster sizes, again together with the DOS of bulk Fe crystal. Our results for a 9-atom cluster differ considerably from calculations of Lee *et al.*,⁶ who use a symmetrized linear combination of Gaussian orbitals as basis functions. For the majority-spin states of the 27-atom cluster, there is a fair agreement of our results and calculations of Pastor *et al.*,¹ while for spin-minority states this agreement is worse. Generally, one can see from Figs. 12 and 13 that the convergence of the DOS of the whole cluster to the bulk is significantly faster than the convergence of the central atom alone. This may be surprising, as the central atom ought to be the “most bulklike” of all atoms in any cluster and so one would naturally expect that convergence towards bulk characteristics would be first observed just for this atom. The reason for different convergence properties of the DOS of whole clusters and of the DOS of individual atoms of the same clusters is the fact that when DOS curves of several inequivalent atoms are superposed, the sharp structures in the DOS get smeared as they are generally located at different energies for different atoms. Hence the resulting combined DOS lacks the sharp atomic-like features which characterize the DOS of the central atoms in Fig. 12.

As an illustration how the DOS at individual atoms differs from site to site, we display in Fig. 14 the DOS for three

selected atoms of the 89-atom cluster. The left panel shows the DOS for an atom in the second coordination shell (at 2.87 Å from the center), the middle panel stands for the fifth coordination shell (4.97 Å from the center), and the right panel for the seventh coordination shell (the outermost one, at 6.26 Å from the center). The total DOS per atom of the whole 89-atom cluster is displayed by thick dashed lines in each of the panels for comparison. Generally, it is quite difficult to observe any systematic trends in the DOS when moving from one atomic site to another. In analogy with an oscillatory dependence of μ_{spin} and μ_{orb} on the radial distance (Figs. 1 and 2), the DOS character does not change uniformly when moving farther from the cluster center. Nevertheless, a general tendency to narrowing the local band for atoms close to cluster surface, which can be seen in Fig. 14, is present for all clusters. This trend has been, albeit for a smaller range of cluster sizes, observed also by Yang *et al.*⁵ and Pastor *et al.*¹ In this respect the surface of a spherical cluster resembles the crystal surface, where narrowing of bands also occurs. However, layer-resolved profiles of DOS in clusters and at crystal surfaces significantly differ in details⁶⁴—similarly as in the case with layer-resolved profiles of μ_{spin} and μ_{orb} (see Figs. 6 and 7).

It is interesting to note that for atoms which belong to the same coordination sphere but are inequivalent due to the presence of a magnetization, the corresponding DOS curves are practically identical (within the thickness of the line). This may be a bit surprising, however, it is consistent with the observation that μ_{spin} , which stems from differences between spin-up and spin-down DOS, also hardly differs in these circumstances (as noted in Sec. III A). Nonzero μ_{orb} ,

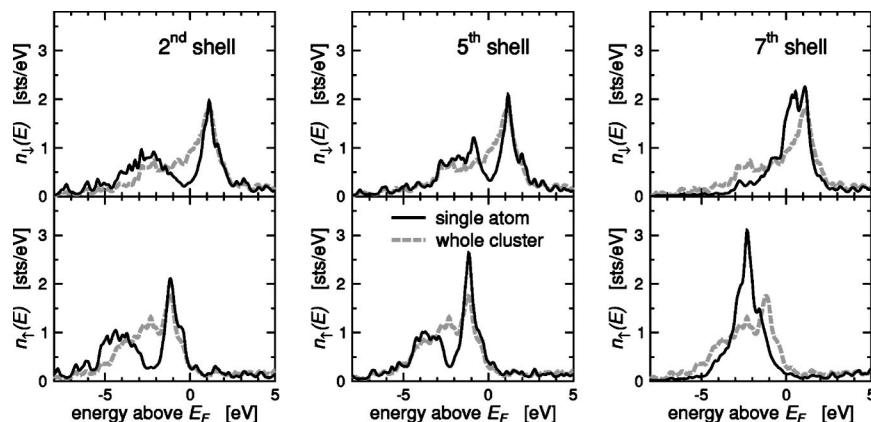


FIG. 14. Spin-polarized DOS at individual atoms of an 89-atom cluster (thin solid lines) compared with DOS averaged over all atoms of that cluster (thick dashed lines). The left panel displays the DOS for an atom of the second coordination shell, the middle panel for an atom of the fifth coordination shell and the right panel for an atom of the seventh (i.e., outermost) coordination shell.

on the other hand, is caused by the small imbalance of the DOS related to the m_l -related states due to the presence of the spin-orbit coupling (m_l stands for the magnetic angular momentum quantum number). Of course the corresponding shifts in energy are quite small.

Let us make finally a note about the angular-momentum character of electron states in clusters. Obviously, the DOS around atoms in clusters has overwhelmingly a d character. However, some minor peaks at the outer edges of the main band may have considerable s or p components, as one can expect from the corresponding atomic electron configuration of a free Fe atom. In particular, e.g., the peaks at $E \approx -7$ eV in DOS around central atom of the 89-atom cluster are almost exclusively of s character. Similar trends were observed for a 15-atom cluster by Yang *et al.*⁵ and Vega *et al.*² The occurrence of these s - and p -character peaks is connected with the still partially atomic character of electron states in clusters; in bulk iron, there are just structureless continuum shoulders, typical for a free-electron DOS, instead of well-resolved peaks below the main d band as found for the clusters. Interestingly, the heights of the s and p peaks in the cluster DOS decrease with increasing distance of the atom from the center of the cluster (we do not present corresponding plots for brevity).

IV. SUMMARY

In free spherical bcc-structured Fe clusters, both μ_{spin} and μ_{orb} are enhanced for atoms close to the cluster surface; their depth profiles exhibit an oscillatory structure. The orbital moments of individual atoms μ_{orb} exhibit quite a strong de-

pendence on the direction of the magnetic field, however, the anisotropy in μ_{orb} averaged over all atoms of a coordination shell is very weak. Some common trends in magnetic profiles of free clusters and of crystal surfaces can be observed (enhancement of μ_{spin} and μ_{orb} at surfaces, Friedel-like oscillations). However, the surface enhancement as well as Friedel-like oscillations of μ_{spin} and μ_{orb} are more pronounced for clusters than for semi-infinite crystals. Spin magnetic moments μ_{spin} in clusters and at crystal surfaces depend linearly on the effective coordination number and on the valence charge. A semiempirical $\mu_{\text{spin}}(N_{\text{eff}})$ relationship is able to account for some features of the measured dependence of the magnetic moment of free clusters on the cluster size. The DOS of atoms in centers of free clusters is characterized by many sharp peaks and even for a 89-atom cluster it still differs substantially from the DOS in the bulk. The combined DOS of whole clusters converges to the bulk DOS more quickly than DOS of atoms in the center of these clusters, due to a mutual cancellation of sharp atomlike peaks.

ACKNOWLEDGMENTS

This work was supported by Project No. 202/04/1440 of the Grant Agency of the Czech Republic and by the Research Training Network ‘‘Computational Magnetoelectronics’’ of the European Commission. In addition, the work was partly funded by the German BMBF (Bundesministerium für Bildung und Forschung) under Contract No. FKZ 05 KS1WMB/1 and by the Deutsche Forschungsgemeinschaft within the Schwerpunktprogramm 1153 ‘‘Cluster in Kontakt mit Oberflächen: Elektronenstruktur und Magnetismus.’’

-
- ¹G.M. Pastor, J. Dorantes-Dávila, and K.H. Bennemann, Phys. Rev. B **40**, 7642 (1989).
²A. Vega, J. Dorantes-Dávila, L.C. Balbás, and G.M. Pastor, Phys. Rev. B **47**, 4742 (1993).
³J.A. Franco, A. Vega, and F. Aguilera-Granja, Phys. Rev. B **60**, 434 (1999).
⁴D.R. Salahub and R.P. Messmer, Surf. Sci. **106**, 415 (1981).
⁵Ch.Y. Yang, K.H. Johnson, D.R. Salahub, J. Kaspar, and R.P. Messmer, Phys. Rev. B **24**, 5673 (1981).
⁶K. Lee, J. Callaway, and S. Dhar, Phys. Rev. B **30**, 1724 (1984).
⁷O. Diéguez, M.M.G. Alemany, C. Rey, P. Ordejón, and L.J. Gallego, Phys. Rev. B **63**, 205407 (2001), and references therein.
⁸A.V. Postnikov, P. Entel, and J.M. Soler, Eur. Phys. J. D **25**, 261 (2003).
⁹R.A. Guirado-López, J. Dorantes-Dávila, and G.M. Pastor, Phys. Rev. Lett. **90**, 226402 (2003).
¹⁰O. Šipr, M. Košuth, and H. Ebert, J. Magn. Magn. Mater. **272–276** P1, 713 (2004).
¹¹S. Ohnishi, A.J. Freeman, and M. Weinert, Phys. Rev. B **28**, 6741 (1983).
¹²C.L. Fu and A.J. Freeman, J. Magn. Magn. Mater. **69**, L1 (1987).
¹³O. Hjortstam, J. Trygg, J.M. Wills, B. Johansson, and O. Eriksson, Phys. Rev. B **53**, 9204 (1996).
¹⁴D. Spišák and J. Hafner, J. Magn. Magn. Mater. **168**, 257 (1997).
¹⁵A.M.N. Niklasson, B. Johansson, and H.L. Skriver, Phys. Rev. B **59**, 6373 (1999).
¹⁶J. Izquierdo, A. Vega, L.C. Balbás, D. Sánchez-Portal, J. Junquera, E. Artacho, J.M. Soler, and P. Ordejón, Phys. Rev. B **61**, 13 639 (2000).
¹⁷V. Popescu, H. Ebert, B. Nonas, and P.H. Dederichs, Phys. Rev. B **64**, 184407 (2001).
¹⁸J. L. Rodríguez-López, J. Dorantes-Dávila, and G.M. Pastor, Phys. Rev. B **57**, 1040 (1998).
¹⁹O. Eriksson, G.W. Fernando, R.C. Albers, and A.M. Boring, Solid State Commun. **78**, 801 (1991).
²⁰I.M.L. Billas, J.A. Becker, A. Châtalain, and W.A. de Heer, Phys. Rev. Lett. **71**, 4067 (1993); I.M.L. Billas, A. Châtalain, and W.A. de Heer, J. Magn. Magn. Mater. **168**, 64 (1997).
²¹J. Guevara, F. Parisi, A.M. Llois, and M. Weissmann, Phys. Rev. B **55**, 13 283 (1997).
²²P.J. Jensen and K.H. Bennemann, Z. Phys. D: At., Mol. Clusters **35**, 273 (1995).
²³J. Zhao, X. Chen, Q. Sun, F. Liu, and G. Wang, Phys. Lett. A **205**, 308 (1995).
²⁴F. Aguilera-Granja, J.M. Montejano-Carrizales, and J.L. Morán-López, Phys. Lett. A **242**, 255 (1998).
²⁵For a review see, e.g., J. Stöhr, J. Electron Spectrosc. Relat. Phenom. **75**, 253 (1995).

- ²⁶K.W. Edmonds, C. Binns, S.H. Baker, S.C. Thornton, C. Norris, J.B. Goedkoop, M. Finazzi, and N.B. Brookes, *Phys. Rev. B* **60**, 472 (1999).
- ²⁷K.W. Edmonds, C. Binns, S.H. Baker, M.J. Maher, S.C. Thornton, O. Tjernberg, and N.B. Brookes, *J. Magn. Magn. Mater.* **231**, 113 (2001).
- ²⁸P. Ohresser, G. Ghiringhelli, O. Tjernberg, N.B. Brookes, and M. Finazzi, *Phys. Rev. B* **62**, 5803 (2000).
- ²⁹P. Ballone and R.O. Jones, *Chem. Phys. Lett.* **233**, 632 (1995).
- ³⁰A.N. Andriotis and M. Menon, *Phys. Rev. B* **57**, 10 069 (1998).
- ³¹S.H. Vosko, L. Wilk, and M. Nusair, *Can. J. Phys.* **58**, 1200 (1980).
- ³²V. Ozoliņš and M. Körling, *Phys. Rev. B* **48**, 18 304 (1993).
- ³³M. Battocletti, H. Ebert, and H. Akai, *Phys. Rev. B* **53**, 9776 (1996).
- ³⁴I. Galanakis, S. Ostanin, M. Alouani, H. Dreyssé, and J.M. Wills, *Phys. Rev. B* **61**, 599 (2000).
- ³⁵R. Hafner, D. Spišák, R. Lorenz, and J. Hafner, *Phys. Rev. B* **65**, 184432 (2002).
- ³⁶H. Ebert, in *Electronic Structure and Physical Properties of Solids*, edited by H. Dreyssé (Springer, Berlin, 2000), p. 191.
- ³⁷H. Ebert, The Munich SPR-KKR package, version 2.1.1, <http://olymp.cup.uni-muenchen.de/ak/ebert/SPRKKR>, 2002.
- ³⁸M. Cook, D.A. Case, computer code XASCF, Quantum Chemistry Program Exchange, Indiana University, Bloomington, 1980.
- ³⁹O. Šipr and A. Šimůnek, *J. Phys.: Condens. Matter* **13**, 8519 (2001).
- ⁴⁰O. Šipr and H. Ebert, *Czech. J. Phys.* **53**, 55 (2003).
- ⁴¹L. Szunyogh, B. Újfalussy, P. Weinberger, and J. Kollar, *Phys. Rev. B* **49**, 2721 (1994).
- ⁴²R. Zeller, P.H. Dederichs, B. Újfalussy, L. Szunyogh, and P. Weinberger, *Phys. Rev. B* **52**, 8807 (1995).
- ⁴³T. Oda, A. Pasquarello, and R. Car, *Phys. Rev. Lett.* **80**, 3622 (1998).
- ⁴⁴D. Hobbs, G. Kresse, and J. Hafner, *Phys. Rev. B* **62**, 11 556 (2000).
- ⁴⁵G. Kresse and J. Hafner, *Phys. Rev. B* **47**, 558 (1993); G. Kresse and J. Furthmüller, *ibid.* **54**, 11 169 (1996).
- ⁴⁶J. Minár (private communication).
- ⁴⁷A.P. Cracknell, *J. Phys. C* **2**, 1425 (1969).
- ⁴⁸P. Strange, H. Ebert, J.B. Staunton, and B.L. Gyorffy, *J. Phys.: Condens. Matter* **1**, 3947 (1989).
- ⁴⁹P. Bruno, *Phys. Rev. B* **39**, 865 (1989).
- ⁵⁰G.M. Pastor, J. Dorantes-Dávila, Š. Pick, and H. Dreyssé, *Phys. Rev. Lett.* **75**, 326 (1995).
- ⁵¹H. Ebert and M. Battocletti, *Solid State Commun.* **98**, 785 (1996).
- ⁵²P. Gambardella, S. Rusponi, M. Veronese, S.S. Dhesi, C. Grazioli, A. Dallmeyer, I. Cabria, R. Zeller, P.H. Dederichs, K. Kern, C. Carbone, and H. Brune, *Science* **300**, 1130 (2003).
- ⁵³P. Carra, B. T. Thole, M. Altarelli, and X. Wang, *Phys. Rev. Lett.* **70**, 694 (1993).
- ⁵⁴C. Ederer, M. Komelj, and M. Fähnle, *Phys. Rev. B* **68**, 052402 (2003).
- ⁵⁵N. Papanikolaou, B. Nonas, S. Heinze, R. Zeller, and P.H. Dederichs, *Phys. Rev. B* **62**, 11 118 (2000).
- ⁵⁶M.S.S. Brooks, *Physica B & C* **130**, 6 (1985).
- ⁵⁷O. Eriksson, B. Johansson, R.C. Albers, A.M. Boring, and M.S.S. Brooks, *Phys. Rev. B* **42**, 2707 (1990).
- ⁵⁸H. Ebert and M. Battocletti, *Solid State Commun.* **98**, 785 (1996).
- ⁵⁹V.I. Anisimov, F. Aryasetiawan, and A.I. Lichtenstein, *J. Phys.: Condens. Matter* **9**, 767 (1997).
- ⁶⁰H. Ebert, A. Perlov, and S. Mankovsky, *Solid State Commun.* **127**, 443 (2003).
- ⁶¹L.M. Falicov and G.A. Somorjai, *Proc. Natl. Acad. Sci. U.S.A.* **82**, 2207 (1985); A.J. Freeman and R.Q. Wu, *J. Magn. Magn. Mater.* **100**, 497 (1991); F. Liu, M.R. Press, S.N. Khanna, and P. Jena, *Phys. Rev. B* **39**, 6914 (1989).
- ⁶²D. Tománek, S. Mukherjee, and K.H. Bennemann, *Phys. Rev. B* **28**, 665 (1983).
- ⁶³G.M. Pastor, J. Dorantes-Dávila, and K.H. Bennemann, *Chem. Phys. Lett.* **148**, 459 (1988).
- ⁶⁴O. Šipr, M. Košuth, and H. Ebert, *Surf. Sci.* **566–568**, 268 (2004).